iScience

CellPress
OPEN ACCESS

Article

A stochastic model of homeostasis: The roles of noise and nuclear positioning in deciding cell fate

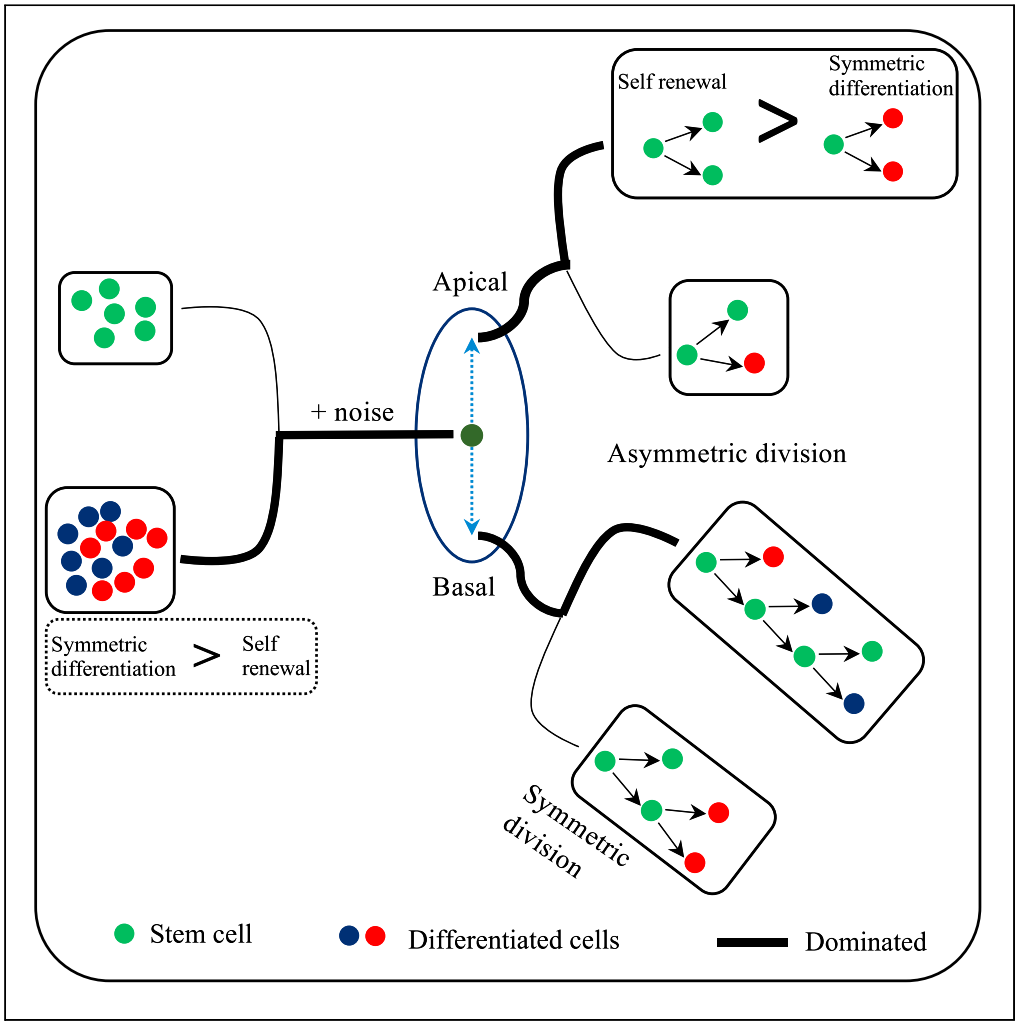

Amit Jangid,
Suriya Selvarajan,
Ram Ramaswamy

amitjangid050@gmail.com

Highlights

Nucleus position biases the cell fate decision by controlling the transcription factors

Apical nuclei prefer symmetric division and basal nuclei favor asymmetric division

Noise in the nucleus position leads to more differentiated cells

Jangid et al., iScience 24, 103199
October 22, 2021 © 2021
https://doi.org/10.1016/j.isci.2021.103199

iScience

CellPress
OPEN ACCESS

Article

A stochastic model of homeostasis: The roles of noise and nuclear positioning in deciding cell fate

Amit Jangid,[1,4,*] Suriya Selvarajan,[2] and Ram Ramaswamy[3]

SUMMARY

We study a population-based cellular model that starts from a single stem cell that divides stochastically to give rise to either daughter stem cells or differentiated daughter cells. There are three main components in the model: nucleus position, the underlying gene-regulatory network, and stochastic segregation of transcription factors in the daughter cells. The proportion of self-renewal and differentiated cell lines as a function of the nucleus position which in turn decides the plane of cleavage is studied. Both nuclear position and noise play an important role in determining the stem cell genealogies. We have observed both long and short genealogies in model simulation, and these compare well with experimental results from neuroblast and B-cell division. Symmetric divisions are observed in apical nuclei, while asymmetric division occurs when the nucleus is toward the base. In this model, the number of clones decreases over time, although the average clone size increases.

INTRODUCTION

A fundamental question in developmental biology concerns the manner in which genetically similar cells give rise to distinct fates during development, and the balance between self-renewal and differentiation, which in turn maintains homeostasis. One prominent mechanism for maintaining long-term homeostasis is through asymmetric cell division that results in one stem and one differentiated daughter cell at each division (Venkei and Yamashita, 2018; Zakrzewski et al., 2019). The alternative is either uncontrolled growth with possible tumorigenesis or tissue degeneration (Morrison and Kimble, 2006; Chen et al., 2016; Berika et al., 2014). Symmetric cell division, on the other hand, leads to two daughter cells that have the same fate, both stem or both differentiated (Lee et al., 2006; Albertson and Doe, 2003; Caussinus and Gonzalez, 2005). Two distinct regulatory pathways appear to play a role in deciding whether daughter cells are self-renewing or differentiated (Horvitz and Herskowitz, 1992; Broadus and Doe, 1997; Inaba and Yamashita, 2012). Specific proteins in the intrinsic mechanism determine cell fate by segregating unevenly in daughter cells; this process is stochastic (Doe and Bowerman, 2001; Yu et al., 2006; Venkei and Yamashita, 2018). Alternately, external factors can decide cell fate by delivering short-range molecules (proteins) (Losick et al., 2011) that communicate between cells by activating or blocking specific transcriptional networks that decide cell fate (Venkei and Yamashita, 2018; Morrison and Spradling, 2008; Losick et al., 2011). Through the so-called intrinsic mechanism (Neumüller and Knoblich, 2009), daughter cells appear to be different in shape, size, and concentration of transcription factors while in the niche mechanism (Morrison and Spradling, 2008; Losick et al., 2011) daughter cells have the same shape, size, and transcription factors. Cell division is an extremely well-studied and complex process that consists of several steps (Betschinger and Knoblich, 2004; Li, 2013). A polarity axis is set up due to the localization of specific types of proteins along the apical-basal axis of cell (El-Hashash and Warburton, 2011; Doe and Bowerman, 2001; Knoblich, 2001; Yu et al., 2006; Yuan et al., 2012; Götz and Huttner, 2005). This axis controls the interactions between microtubules and the cortex, resulting in differential torques on the mitotic spindles and this leads to different shapes and orientation of the spindles (El-Hashash and Warburton, 2011; Gönczy, 2002; Grill et al., 2001; Neumüller and Knoblich, 2009; Abrash and Bergmann, 2009). Transcription factors segregate differentially in different parts of the parent cell, and this results in different concentrations of proteins in daughter cells (El-Hashash and Warburton, 2011; Kaltschmidt et al., 2000; Konno et al., 2008; Delaunay et al., 2014, 2015; Haydar et al., 2003).

Cell fate is controlled, in general, by a combination of gene expression and intrinsic or extrinsic noise. In considering the dynamics of the process, a useful and early suggestion made by Waddington

[1]School of Computational and Integrative Sciences, Jawaharlal Nehru University, New Delhi 110067, India

[2]Department of Theoretical Physics, Tata Institute of Fundamental Research, Mumbai 400005, India

[3]Department of Chemistry, Indian Institute of Technology Delhi, New Delhi 110016, India

[4]Lead contact

*Correspondence: amitjangid050@gmail.com

https://doi.org/10.1016/j.isci.2021.103199

(Waddington, 1957) was to consider the state of the cell as a dynamical attractor (Enver et al., 2009; Huang et al., 2005; Chang et al., 2008; Losick and Desplan, 2008; Perez-Carrasco et al., 2016, 2018; Pokhilko et al., 2018; Zhou and Huang, 2011). Viewed as a dynamical system, the gene-regulatory network (GRN) can have several attractors in the phase space, each corresponding to a different cell type, and each cell type is decided by a different set of genes/proteins at the population level. From a dynamical systems point of view, therefore, differentiation can be considered as a transition from one attractor to another, the transition being driven by several factors. Many regulatory networks can show complex dynamical states – simple examples being genetic switches (Gardner et al., 2000; Zhou and Huang, 2011; Huang et al., 2007; Perez-Carrasco et al., 2018) that can even show multistability, namely the coexistence of several distinct dynamical states. Another determinant of the outcome is the position of the nucleus. Recent studies of an early mouse embryo (Ajduk et al., 2014; Wodarz and Huttner, 2003), for example, suggest that the position of the nucleus can alter cell fate by controlling the division plane. When toward the apical side, divisions tended to be more symmetric, and when the nucleus was nearer the basal portion, more asymmetric divisions were seen. Increased expression of Cdx2, which controls movement of the nucleus, increases aPKC expression and this then leads to symmetric division (Ajduk et al., 2014). A third factor is the differential shape and size of daughter cells which have different concentration of expressed proteins (Neumüller and Knoblich, 2009). In the absence of intrinsic noise proteins are expressed in a correlated manner (Elowitz et al., 2002); by reducing the noise in ComK, the protein that regulates competence for DNA uptake, it is possible to decrease the number of competence cells (Maamar et al., 2007). This suggests that sufficient noise may alter cell fate. Taken together, these observations suggest that these factors, namely intrinsic noise, nucleus position, segregation of transcription factors in daughter cells and the GRN play a crucial role in deciding cell fate.

Indeed, the role of noise in deciding cell fate is known, for example, by altering gene expression levels in daughter cells which either activate or block particular pathways to switch the cell identity (Elowitz et al., 2002; Maamar et al., 2007). In the model (Serbanescu et al., 2020), it has observed that cell size variability depends on the balance between ribosomes and division protein which depends on nutrient availability. Gene expression boundary sharpening controlled by morphogens shows that mutual repressed self-activation network is more robust than others against parameter perturbation (Li et al., 2018). A noise-driven cell differentiation model (Safdari et al., 2020) that uses a GRN with two mutually inhibiting transcription factors shows an increasing number of differentiated cells as division plane deviate from center of the cell. And the differentiation reduces as noise level decreases. Noise also shows spatiotemporal heterogeneity (Safdari et al., 2020). Several models of noise-driven transitions have been investigated, as for instance the control of stem cell and progenitor populations by noise intensity (Hoffmann et al., 2008), transitions in a toggle switch controlled by noise with different spectral characteristics such as white noise, colored noise, Lévy noise (Wang et al., 2007, 2015; Xu et al., 2016), as well as transitions driven by external signals (Perez-Carrasco et al., 2018; Lai et al., 2004; Stockholm et al., 2010).

Thus the factors that play a crucial role in deciding cell fate are intrinsic noise, nucleus position, segregation of transcription factors in daughter cells and the GRN. In the present work, we propose a population-based stochastic model of cell division starting from a single stem cell which includes these components such as nucleus position, the stochastic partitioning of transcription factors and GRN. The model is fully driven by intrinsic noise. In the model, we explore how nucleus position regulates symmetric and asymmetric cell division, as well as the plane of cleavage which is controlled by nucleus position, and how these change the relative fractions of cell types. We also study the effect of noise in nucleus position on the relative fractions of cell types. Different types of genealogies have been studied along with cell line behavior in individual generation of cell division as a function of nucleus position and generation. We also study as is the average number of clones and average clone size as a function of time (Stine and Matunis, 2013; Klein and Simons, 2011; Hara et al., 2014). Coarse graining gives a simpler Markov model which shares some important features of the full dynamical model.

The paper is organized as follows. Below we first discuss some experimental evidence for the different aspects of the model, namely the GRN, as well as the internal dynamical processes such as cell growth, division, and segregation of transcription factors. The dynamical model is presented, and the coarse-graining procedure to obtain the simpler Markov model is discussed. We then discuss the bimodal distribution of stem cells obtained from the present model simulations. This is followed by a discussion and conclusions of our results.

Evidences supporting model components

In the study of mouse embryo, it has observed that nucleus position is an import factor in deciding the division plane which divides the transcription factors in daughter cells respective to their volume (Ajduk et al., 2014). Based on equal and unequal distribution of transcription factors, daughter cells meet their fate. Apical positioning of nucleus enhances symmetric division and basal positioning lead to more asymmetric divisions. There is experimental evidence for a high-dimensional stable attractor in a model of transcription (Huang et al., 2005); the attractor represents a distinct cell fate with different level of transcription factors, with differentiation being seen as a transition from one attractor to another. The synthetic toggle switch first proposed (Gardner et al., 2000) consisted of two transcription factors (X, Y) mutually repressing each other, with overexpression of either suppressing the expression of other, which in turn influence the outcome. This system can thus be seen as an example of two coexisting attractors. An instance where there are three different cell states is in the case of PU.1 and GATA-1 transcription factors in blood cells: different levels of these proteins (Okuno et al., 2005; Tsai et al., 1991) leads to different cell states: (a) myeloid cells, with PU.1 > GATA-1, (b) erythroid cells, with GATA-1 > PU.1 and (c) common myeloid progenitor cells, with GATA-1 ≈ PU.1 (Huang et al., 2007; Enver et al., 2009). The synthetic circuits of these two transcription factors are inhibited by each other while being self-activating (Okuno et al., 2005; Tsai et al., 1991; Huang et al., 2007). A regulatory network consisting of Cdx2/Oct4, GATA6/Nanog, Ptf1a/Nkx6, and Pax3/Foxc2 (Zhou and Huang, 2011) also shows three different cell states. It has observed (Elowitz et al., 2002) that in the presence of intrinsic and extrinsic noise (measured by cyan fluorescent protein and yellow fluorescent protein), in a single cell, results in the variation of gene expression and in another experiment (Maamar et al., 2007) it has showed that variation in gene expression can lead to transitions between alternative states of gene expression.

The dynamical model

The regulatory network that we have used here (Figure 1A) has three different cell states and can be considered as representative. We consider a pair of transcription factors denoted X and Y that mutually inhibit each other while being self-activating. The stoichiometric equations are straightforward to obtain (Table 1) and through standard analysis, it can be seen that in this system there are a large number of dynamical attractors for any set of parameters. Three are of special importance here and are indicated in Figure 1B); they are fixed point attractors and correspond to two distinct cell fates. When the asymptotic values X^* and Y^* are identical, this corresponds to the cell type S, and when the asymptotic values of X and Y are unequal, one has type A ($X^*>Y^*$) or type B ($Y^*>X^*$). In our interpretation, type S corresponds to a stem cell, while types A and B are differentiated cells. The basins of attraction for these three types of cells are shown in Figure 1C for a typical choice of parameters. Other regulatory networks can also be incorporated in such models (Perez-Carrasco et al., 2016, 2018; Pokhilko et al., 2018); combinations of the toggle switch (Perez-Carrasco et al., 2018) and repressilator (Perez-Carrasco et al., 2018) which can have different steady states, showing richer dynamics.

The dynamical equations corresponding to the above model are studied in the usual manner. Starting from an initial volume V_0, we take a single initial stem cell with nucleus at position P_0 and a random initial concentrations of X and Y corresponding to stem cell attractor. Assuming the presence of sufficient chemicals for proper cell growth, the cell can be taken to grow at an exponential rate whereas in the absence of adequate nutrients, the rate of growth seems to be linear. We have used the Gillespie algorithm (Lu et al., 2004) in our simulations with the volume depends on time as $V=V_0 exp^{\lambda t}$. The decay rate μ is independent of volume, but the other rates (the autocrine and paracrine terms) are volume dependent (see Table 1). The volume-dependent rates give rise to additional complexity in the dynamics (Lu et al., 2004).

The plane of cleavage is decided by the position of the nucleus at the time of cell division, as well as by the segregation of transcription factors (Betschinger and Knoblich, 2004; Li, 2013; Ajduk et al., 2014; Wodarz and Huttner, 2003). The parameter P (Figure 2 top box) is the fraction of the distance along the principal axis of the cell (measured from the base) at which the nucleus is situated. As soon as the volume reaches a threshold V_C, the cell divides, with probability P along the vertical plane, and with probability 1-P along the horizontal. Transcription factors are also distributed stochastically in the two daughter cells, proportional to the relative volumes, and the nucleus position is set at random in the newly created daughter cells as well. Starting from a single stem cell as the root of the genealogical tree, the system is propagated in time as follows. The cell grows in size as described above and once the volume exceeds V_C, division takes

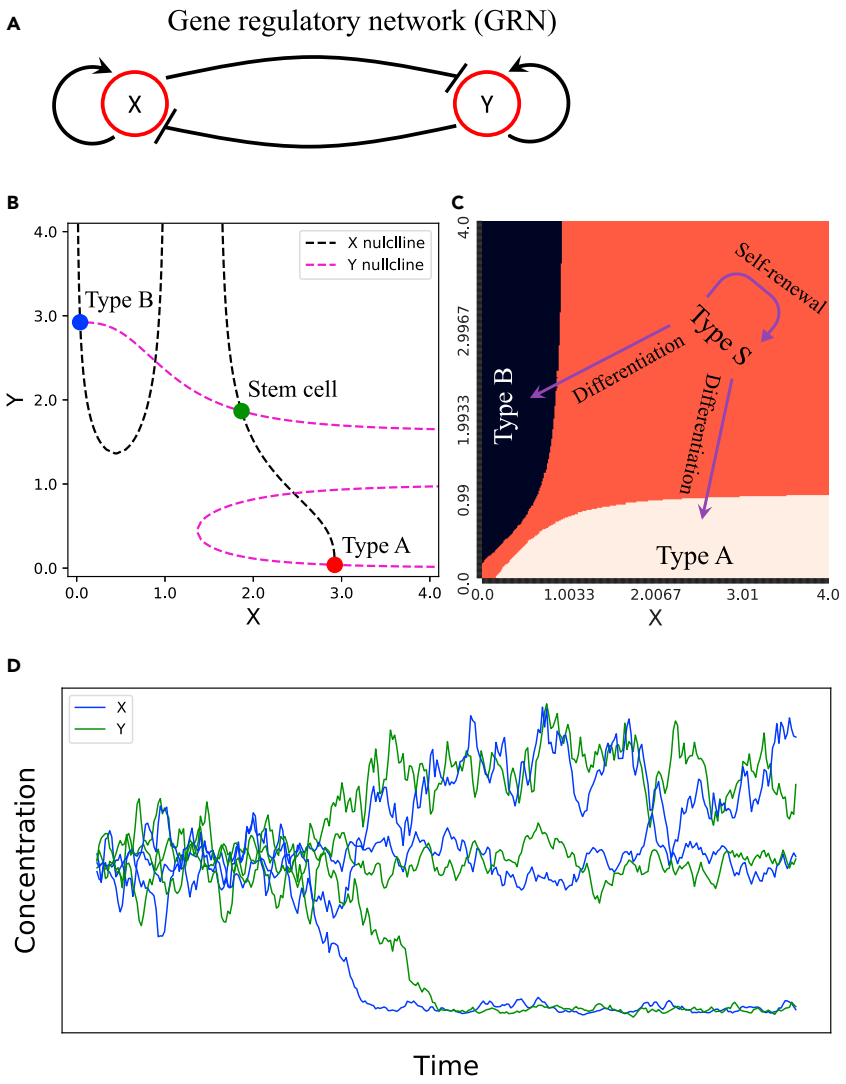

Figure 1. Gene regulatory network and basin of attraction

(A) Gene regulatory network with two transcription factors X, and Y inhibiting each other and self-activating.

(B) Nullcline showing three different attractor corresponding to three different cell type S, A, and B.

(C) Basin of attraction in which three different shaded region correspond to three different cell types S, A, and B in phase space (*X* and *Y* are concentration). Blue arrow from S to S represents self-renewal, while arrow toward A, and B region correspond to differentiation due to internal or external noise. S represents stem cell, and A and B represent differentiated cells.

(D) shows three different time course of transcription factors X, and Y corresponding to (C).

See Figure S9 for quasi-potential.

place. Equations 1 and 2 of the regulatory network are used for the evolution of transcription factors in each of the daughter cells. If the daughter cells are stem, then further division can take place. Data for each cell are collected and summarized in a genealogical tree with averaging over 500 cell divisions; see Figure 2 for a representative result.

The average clone size and clone number as a function of time is also monitored. We consider a simple case of clonal competition (heterogeneous evolution of clones) in which a stem cell is replaced, based on its division time, in the different pool of clones. The stem cell with the earliest time of division is stochastically lost and will be replaced by daughter cells, via symmetric renewal (gain in stem cell by one), symmetric

Table 1. Reactions pertaining to the regulatory network shown in Figure 1A

No.	Reaction	Model parameters
1.	S → X	$r_1 = \alpha_1 \frac{X^n}{1+X^n} + \beta_1 \frac{1}{1+Y^m}$
2.	S → Y	$r_2 = \alpha_2 \frac{Y^m}{1+Y^m} + \beta_2 \frac{1}{1+X^n}$
3.	X → P	$r_3 = \mu_X$
4.	Y → P	$r_4 = \mu_Y$

X and *Y* are transcription factors, *S*, and *P* are substrate and products, respectively.

differentiation (loss in stem cell by one), and asymmetric renewal (no loss or gain). In this competition, there is no interaction among members of the set.

RESULTS

We study the dynamics of the proposed population model for different nucleus positions such as 0.1, 0.5, and 0.8. We have taken four different cases of cell division namely *horizontal*, *vertical*, *mixed*, and *random*. (1) *Horizontal*: in each cell division, plane of cleavage will be horizontal through nucleus. (2) *Vertical*: irrespective of the nucleus position plane of cleavage will be vertical. Each daughter cell will be having half of mother cell volume. (3) *Mixed case*: in each cell division plane of cleavage will be decided by nucleus position *P*. Volume and transcription factors will also be decided by nucleus position. (4) *Random case*:

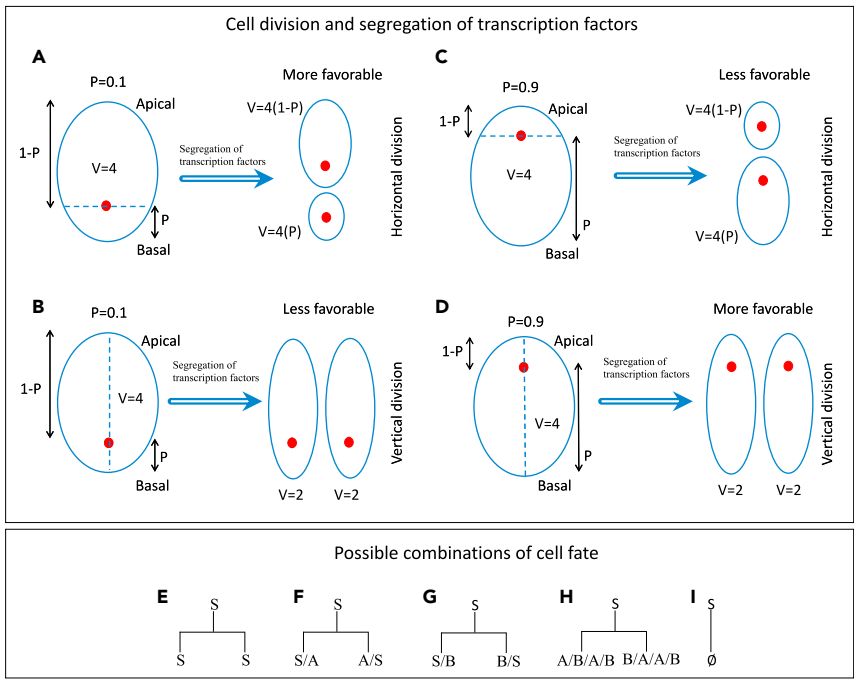

Figure 2. Cell division and segregation of transcription factors (top box)

Schematic diagram of a stem cell for horizontal and vertical division for different nucleus positions (red dots) and segregation of transcription factors in daughter cells (top box). Horizontal and vertical dashed (blue) line through the nucleus correspond to horizontal and vertical division of cell, respectively. *P* is the height of nucleus from the base, and 1−*P* is from the apex. For p = 0.1, horizontal division (A) is more favorable than vertical division (B), whereas for p = 0.9, vertical division (C) is more favored than asymmetric division (D). Possible combinations of daughter cell fate in each cell division (bottom box). (E) and (H) correspond to symmetric renewal and symmetric differentiation respectively whereas (F) and (G) correspond to asymmetric division and (I) corresponds to cell death (though we did not count cell death throughout the model). S indicates stem cell, A and B indicate differentiated cell, and ∅ indicates a dead cell. See Figure S8 for Markov chain.

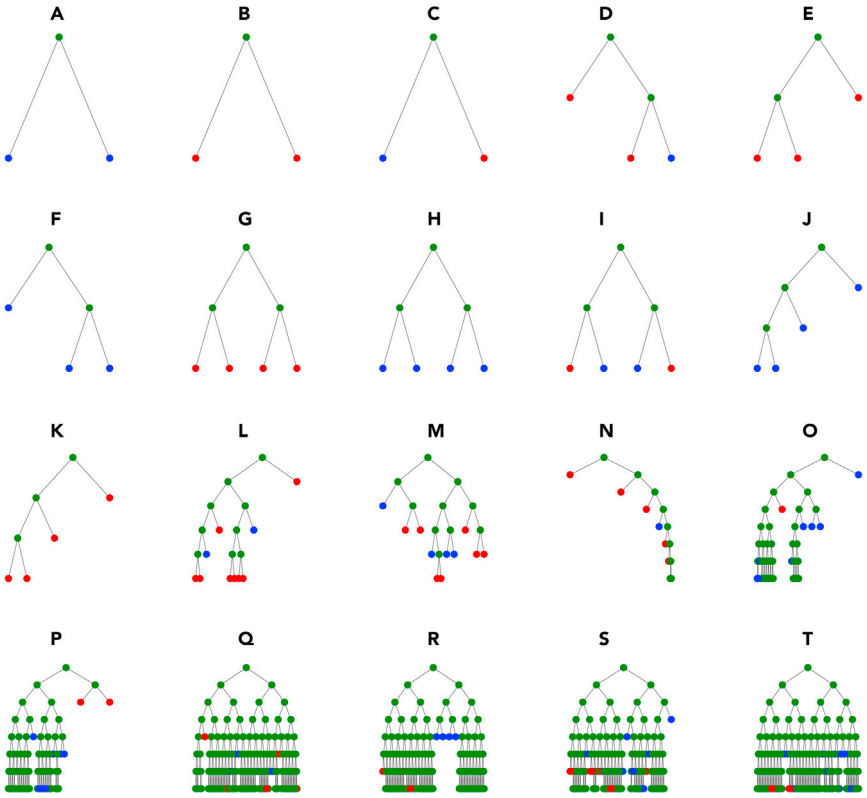

Figure 3. Genealogies obtained from model simulation

Short terminated and non-terminated genealogies pattern for different cases with symmetric and asymmetric division. Panel (A–M) are the short terminated genealogies, while rest (N-T) are the larger genealogies which further divide. We have shown here maximum 7 generations. Red, blue, and green nodes correspond to cell type A, and type B, and stem cell, respectively.

In this case, horizontal and vertical both will be having same probability. We have also introduced noise in nucleus position in each case and compared the results.

Model simulation

Short and non-terminating genealogies

Short and long non-terminated genealogies were first observed in the central nervous system with symmetric and asymmetric trees and in neural stem cells (Qian et al., 1998, 2000; Costa et al., 2011). Long (non-terminated) genealogies were the result of symmetric division (self-renewal), whereas short genealogies were the result of asymmetric division or symmetric differentiation. The proposed model also mimics the behavior of genealogies for different nucleus position, plane of cleavage, and noise showing symmetric and asymmetric division pattern (Figure 3). Red, blue, and green nodes correspond to type A, type B, and stem cell, respectively. Figures 3A–3C are the genealogies terminating after the first generation in which Figures 3A and 3B are symmetric having differentiated daughter cells with similar fates, whereas Figure 3C is asymmetric with two different differentiated daughter cells. Figures 3D–3I are the genealogies terminating after two generations being Figures 3D–3F asymmetric, and Figures 3G–3I symmetric. Figures 3J–3M are terminating trees after three to five generation being all asymmetric. The remaining Figures 3N–3T represent non-terminating genealogies having stem cells as leaf nodes. With increasing tree size the probability of having symmetric genealogies decreases due to three different cell types. Few genealogies go beyond 50 generations (in case of horizontal division with noise in nucleus position). We have also observed that vertical division leads to more non-terminating genealogies than horizontal division because of an increase in the number of stem cells. In every short terminated genealogy, the number of stem cells goes to zero.

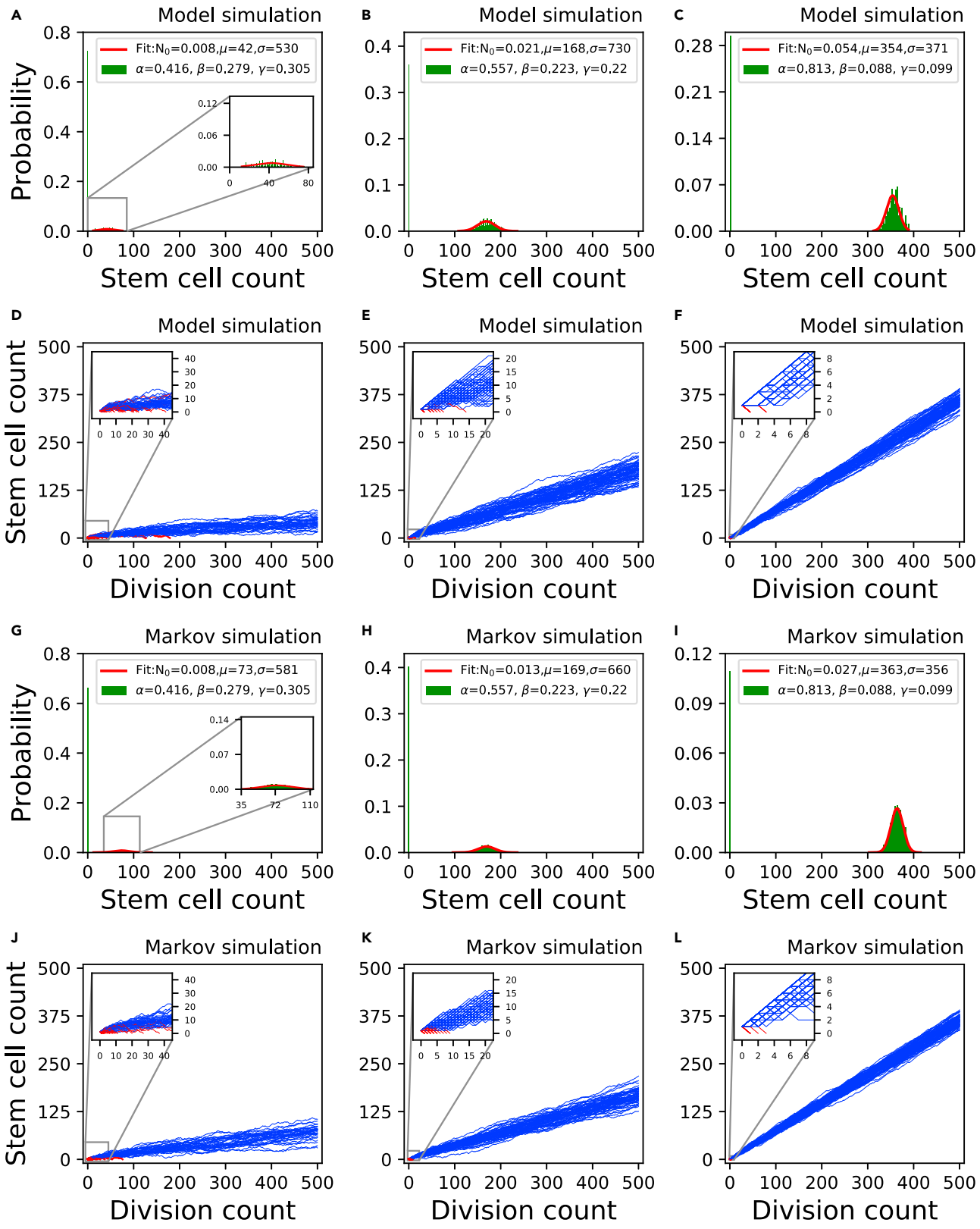
A
Model simulation
Fit:N0=0.008,μ=42,σ=530
α=0.416, β=0.279, γ=0.305
Probability
Stem cell count
B
Model simulation
Fit:N0=0.021,μ=168,σ=730
α=0.557, β=0.223, γ=0.22
Stem cell count
C
Model simulation
Fit:N0=0.054,μ=354,σ=371
α=0.813, β=0.088, γ=0.099
Stem cell count
D
Model simulation
Stem cell count
Division count
E
Model simulation
Division count
F
Model simulation
Division count
G
Markov simulation
Fit:N0=0.008,μ=73,σ=581
α=0.416, β=0.279, γ=0.305
Probability
Stem cell count
H
Markov simulation
Fit:N0=0.013,μ=169,σ=660
α=0.557, β=0.223, γ=0.22
Stem cell count
I
Markov simulation
Fit:N0=0.027,μ=363,σ=356
α=0.813, β=0.088, γ=0.099
Stem cell count
J
Markov simulation
Stem cell count
Division count
K
Markov simulation
Division count
L
Markov simulation
Division count

Figure 4. Bimodal behavior of probability distribution

Top row (A-C) shows probability distribution of stem cell for different set of α, β, and γ calculated over 5000 samples from model simulation. Second row (D-F) represents stem cell population as a function of cell division count corresponding to the parameter used in top row for 100 trials. Third row (G-I) represents same probability distribution for same set of α, β, and γ from Markov simulation calculated in top row, and bottom row (J-L) represents stem cell population as a function of cell division count from Markov simulation corresponding to the parameters calculated in top row. Blue and red color correspond to non-terminating, and terminating genealogies. Gaussian fit for top and third row is shown in red color for standard parameters N_0, μ, σ. See Figure S8 for Markov chain.

Bimodal distribution of stem cell

Observing short and non-terminating genealogies from experiments suggests that there is possibility of two modes of cell distribution each with different mean and variance. We have plotted stem cell distribution for different cases which shows bimodal distribution (Figures 4A–4C) and also observed increasing pattern of stem cell population as a function of division count (Figures 4D–4F). In the cell division, there are three different possibilities self-renewal, symmetric differentiation, and asymmetric differentiation. We can define three parameters (α,β,γ) which corresponds to these events, respectively. To compare the above results (model simulation), we device an another simpler model (Markov) which can give the probability of a state having certain number of stem cells after n such cell divisions (STAR Methods), and the parameters can be found for large samples obtained from model simulation. So from coarse graining we have calculated these three sets of α, β, γ such as (0.416, 0.279, 0.305), (0.557, 0.223, 0.22), and (0.813, 0.088, 0.099) from 5000 samples (Figures 4A–4C, respectively). For same three sets of α, β, γ, we have plotted probability distribution from Markov process (Figures 4G–4I, respectively). Stem cell distribution in Figures 4A and 4B are in very good agreement with distribution in Figures 4G and 4H in the probability of stem cell, and in the range of cells numbers (fitted Gaussian distribution), whereas distribution in Figure 4C gives good agreement in the cell numbers with panel Figure 4I but not in the probability. Cell counts, from model (Figures 4D–4F), is also in good agreement with Markov process (Figures 4J–4L, respectively). Markov approach gives a very simple picture of cell distribution having no nucleus position, while the purposed model gives much rich behavior because of having different types of plane of cleavage, nucleus position, and GRN.

Nucleus position and noise altering cell fate decision

Cell distribution comparison among similar plane of cleavage

The proposed stochastic model and Markov process both result bimodal distribution of stem cells which are in good agreement. We have plotted the distribution of differentiated cell type A, B, and stem cells for 4 cases (with and without noise in nucleus position) for each 0.1, 0.5, and 0.8 nucleus position (Figure 5 only for nucleus position 0.1, see Figures S1 and S2 for 0.5 and 0.8). In each case of cell division probability and range of cell type A against B is similar in case of noise in nucleus position such as Figure 5A_1 has same range and probability distribution as A_2, same for B_1 v/s B_2, C_1 v/s C_2, D_1 v/s D_2. It is due to the same parameters ($n = m = 3.0$) taken in GRN, which gives the symmetrical nature of cell type A and B from the stem cell attractor (Figures 1B and 1C). In this case, the same noise level results in the same chance of transition, whereas for a different set of parameter values ($n \neq m$), the chance of transitions biases toward one cell type than the other. Noise in nucleus position results in different stem cell range with different probabilities (Figures 5A_3,5B_3,5C_3, and 5D_3) then cell type A and B. Second peak in the cell distribution of stem cells range from 20–70 (Figures 5A_3), 320–400 (B_3), 125–290 (C_3), and 130–220 (D_3) for asymmetric, vertical, mixed, and random case with noise in nucleus position, respectively, while there is sharp peak at zero (first peak) with different probabilities.

The absence of noise in nucleus position, results in the distribution with same probability and range (40–120) of cell type A against B such as Figures 5A_4, 5B_4, 5C_4, and 5D_4 against Figures 5A_5, 5B_5, 5C_5, and 5D_5, respectively. And stem cells also range (second mode) from 320–400 (Figures 5A_6, 5B_6, 5C_6, and 5D_6) in all four cases and also give a sharp peak at zero (first mode). These results suggest that noise in the nucleus position gives lower number of stem cells due to short genealogies, where no-noise results in long non-terminated genealogies with less differentiated cells. There is a larger range of stem cells (second mode, Figure 5B_3) because noise does not change the plane of cleavage as vertical division is independent of nucleus position. Red, blue, and green color in Figure 5 represents differentiated type A, type B, and stem cells, respectively. Similar behavior has observed for nucleus position p = 0.5 and 0.8 shown in Figure S1 and S2, respectively.

Cell distribution comparison among different plane of cleavage

In case of noise in the nucleus position, there are different ranges of cell type A, B, and stem cells (Figures 5A_1–5A_3, 5B_1–5B_3, and 5C_1–5C_3). Random case gives similar range as mixed case (Figures 5C_1–5C_3 and

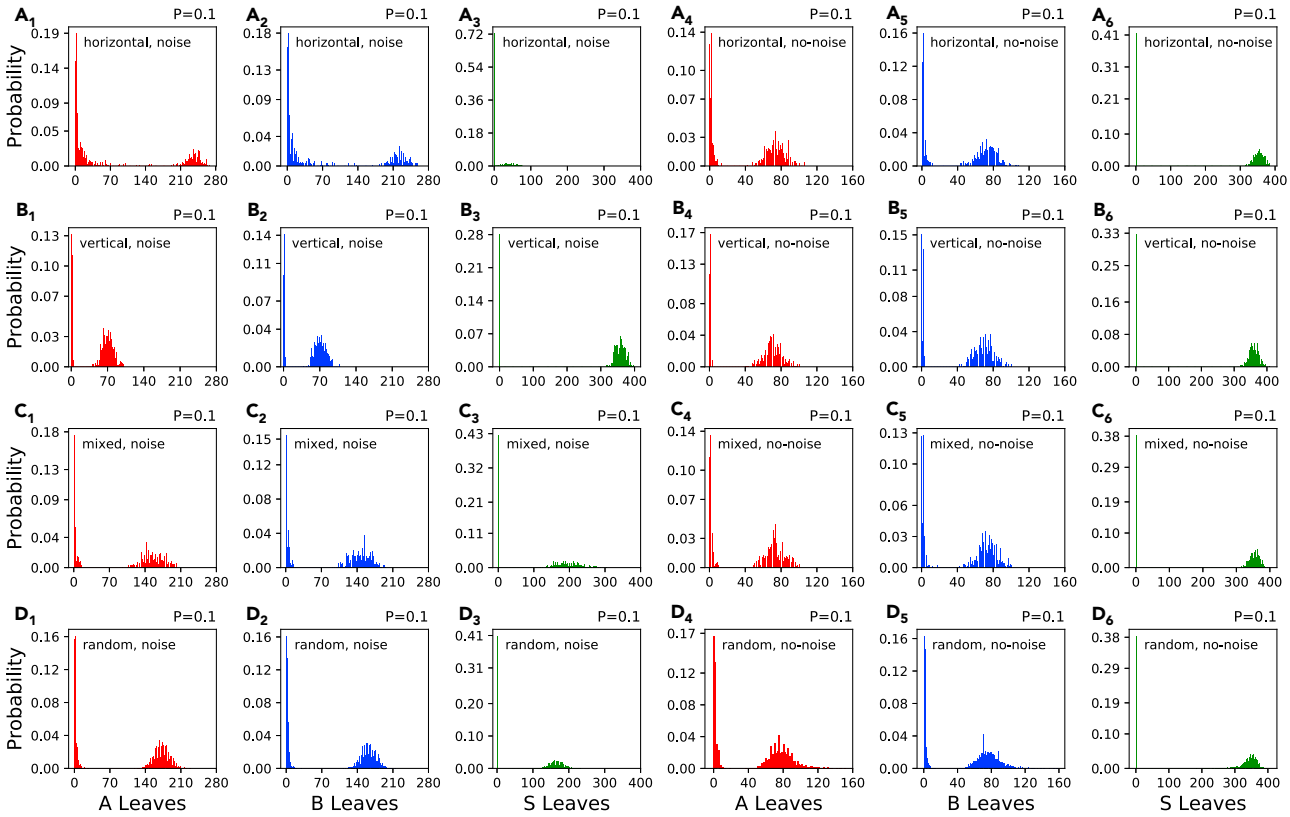

Figure 5. Probability distribution of differentiated cell type A, B, and stem cell S

Probability distribution of cell A (differentiated, red color), B (differentiated, blue color), and S (stem cell as leaf, green color) for all 8 different cases horizontal (A1-A6), vertical (B1-B6), mixed (C1-C6), and random (D1-D6) with noise and without noise in nucleus position, averaged over 5000 samples. In each panel on the top right *P* represents nucleus position, and in the panel, first, and second text represent type of plane of cleavage, and noise in the nucleus position, respectively. See Figures S1 and S2 for nucleus position 0.5 and 0.8 respectively and S7 for p test.

$5D_1$–$5D_3$). Horizontal division gives the largest range of cells A and B (first mode: 0–140, second mode: 140–270) with the lowest range of stem cells (first mode: 0, second mode: 20–70), whereas vertical division gives the lowest range of cells A, and B (first mode: 0–10, second mode: 40–100) with highest range of stem cells (first mode: 0, second mode: 300–400). In case of no-noise, the range of A, B, and stem cells are the same across all four different cases (Figures $5A_4$–$5A_6$, $5B_4$–$5B_6$, $5C_4$–$5C_6$, and $5D_4$–$5D_6$).

Fraction of stem and differentiated cell as a function of nucleus position and noise. We study the fraction of stem cells, Figure 6, for three different nucleus positions (0.1,0.5,0.8) for each case discussed above. Introducing noise in nucleus position results in more differentiated cells and fewer stem cells (Figure 6A). When noise is suppressed, fewer differentiated cells are created (Figure 6E). Highest number of stem cells are created for nucleus position p = 0.5. Vertical divisions, where the nucleus position does not play a role, lead to two similar daughter cells. We find a similar fraction of stem cells for different nucleus positions, as well as differentiated cells irrespective of noise in the nucleus position (Figures 6B and 6F). When there is noise in the nucleus position, the population of stem cells increases. Differentiated cells tend to decrease when the nucleus moves toward the apex (Figure 6C). We have also observed that in this case, the population of differentiated cells tends to be greater than the number of stem cells regardless of nucleus position, indicating more asymmetric division than self-renewal. Similarly, when the nucleus is moved from the basal to apical position (Figure 6G), removing the noise increases stem cells, suggesting that in general, the suppression of noise results in more self-renewal (compare to the nucleus at center Figure S10). In the case of random division there is no significant changes in the population of differentiated and stem cells for different values of nucleus position (Figures 6D and 6H). When the nucleus is close to the apex, there are more daughter cells with similar transcription factors (Figures 6I and J) and therefore eventually similar fates.

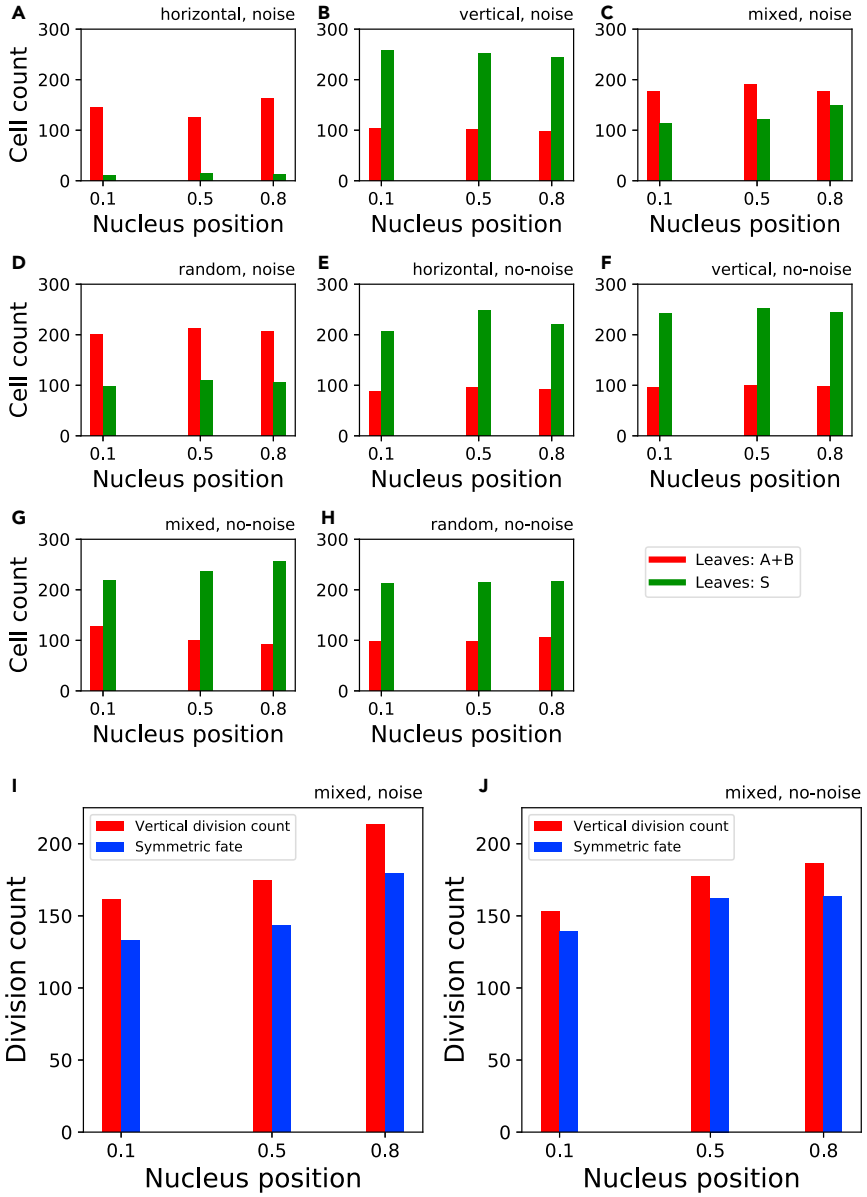

Figure 6. Number of differentiated and stem cells for different plane of cleavages with different nucleus position

Bar plot for number of total differentiated cells (A + B, red color), and total S cells (leaves, green color) for nucleus position 0.1, 0.5 and 0.8 for 8 different cases, averaged over 5000 samples. First and second text on top right in each panel represent plane of cleavage and noise in the cell division respectively. Panels represent the following cases: (A) horizontal (with noise), (B) vertical (with noise), (C) mixed (with noise), (D) random (with noise), (E) horizontal (no-noise), (F) vertical (no-noise), (G) mixed (no-noise), (H) random (no-noise) case. Increasing nucleus position increases symmetric cell division: Number of symmetric cell division (symmetric fate) from total number of vertical division for nucleus position 0.1, 0.5, and 0.8 for mixed cases with (I) and without noise (J), averaged over 5000 samples. If both daughter cells are differentiated (either cell type A, B or combination of A and B) or stem cells, are counted as symmetric division (same fate). First and second text on top right in each panel represent plane of cleavage and noise in the cell division, respectively. See also Figure S10.

Population dynamics of cell over time and generation

We have studied the cell dynamics in different generations as a function of time. Figures 7A–7C represent similar qualitative cell dynamics as observed in experimental studies (Mitchell et al., 2018; Hawkins et al., 2009; Roy et al., 2019; Shokhirev et al., 2015). The dynamic shows that cell counts, green dashed line, starts increasing after

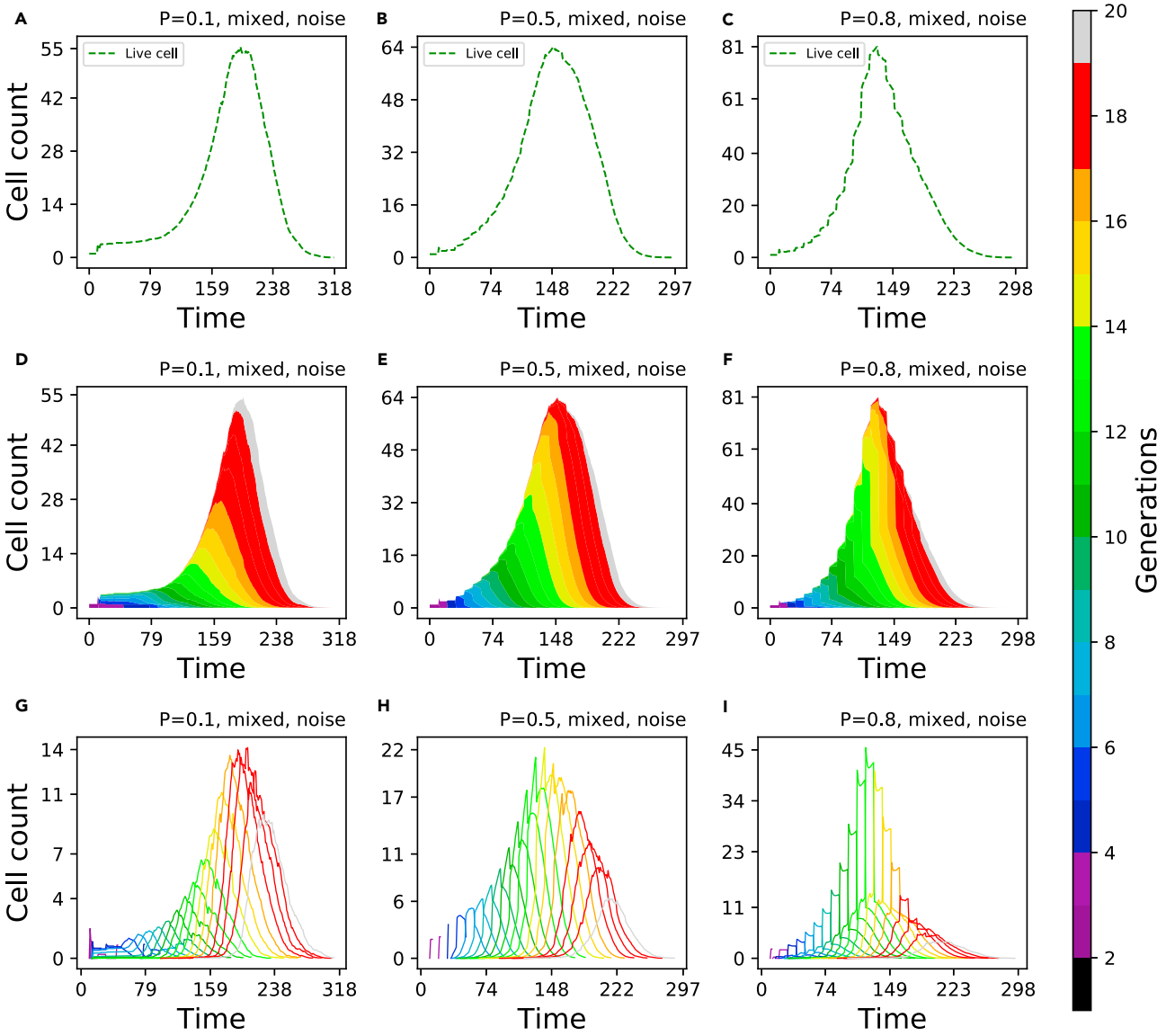

Figure 7. Population dynamics of cell over time

Top row (A-C) displays total live cell dynamics over time. Second (D-F) and third row (G-I) represent stacked area plot of total cell counts with the contribution of each generation (up to 20 generations), and cell counts in individual cell generation respectively. Color spectrum represents for different generations for second and third row. In each panel on the top right *P* represents nucleus position, second, and third text represent type of plane of cleavage, and noise in the nucleus position, respectively. See also Figures S3–S6.

initial cell divisions and reaches up to a certain level followed by a decreasing cell line, Figures 7A–7C for three different nucleus position 0.1, 0.5, and 0.8, respectively. The observations indicate that initially there are more symmetric divisions for certain time intervals, which give more stem cells to divide (overall number of cell increases) and later more symmetric differentiation and asymmetric division, which eventually leads to more specialized cells that do not divide further. For nucleus position 0.1, 0.5, and 0.8 (Figures 7A–7C), the peak value of cell count increase as nucleus position shifts toward apical (55, 64, 81 cell count), and the time where peak has observed shifts toward left side (193, 152, 128). These results suggest that there is an increase in the number of symmetric divisions as nucleus position shifts toward apical portion. Figures 7D–7F represent stacked area plot for individual generation, up to 20 generations, as a function of time. We have observed that cell dynamics in individual generation, Figures 7G–7I, follow Gaussian distribution with different maximum cell number at different time, which are qualitatively similar to experimental observation.

To study the effect of different nucleus position, plane of cleavage, and noise in the nucleus position on cell dynamics, we have plotted cell dynamics for all 24 different conditions (Figure S3). Cell dynamics (thick black line) show common behavior across all panel, that is initially increasing pattern of cell counts followed by a decreasing pattern after attaining a certain threshold. It also suggests that the presence of the noise in nucleus position, keeping nucleus position and plane of cleavage similar, leads to more number of generations and time taken to achieve a certain population level. Such as the number of generations is going beyond 50 in Figure S3A_1 whereas, in Figure S3A_5, a number of generations have observed 17 and time for these two conditions are 747 days and 235 days, respectively. Similar scenario can be observed across different panels of Figure S3. There is no variability in the cell dynamics in each panel across second column and fourth row of Figure S3. Vertical division is independent of nucleus position, and noise so there will be no variability in the cell dynamics (second raw), whereas in Figures S3B_5, S3B_7, and S3B_8, p = 0.5 behave as an attractor in which nucleus position will be 0.5 in daughter cells throughout the divisions which will lead to no variability in cell dynamics. We have also plotted cell dynamics (Figure S4) in an individual generation for different cases, which shows Gaussian distribution. In summary, we have observed three behavior, more symmetric division for apical nuclei, symmetric division takes lesser time to achieve a certain threshold than asymmetric division, and noise increases number asymmetric division (larger number of generations are possible through asymmetric division for certain carrying capacity).

We have plotted the dynamics of maximum cell count in an individual generation for three different nucleus position (Figures S5A–S5C), which shows a Gaussian distribution with fitted parameter values $N_0 = 13.318$, $\mu = 16.202$, $\sigma = 4.04$, suggesting that increasing *P* (toward apical), increases the peak value of the maximum cell count however decreases the generation for that peak value. Figures S5D–S5F represents the probability distribution of cell division showing decaying pattern (Figure S5E showing positive skewed distribution), and Figures S5G–S5I show fraction of undivided cells (Hara et al., 2014). The dynamics of maximum cell count in an individual generation for all 24 conditions have shown in Figure S6, giving similar observations. p test for all 24 possible conditions (Table S1) has shown in Figure S7.

Heterogeneous evolution of clones: Survival clones and average size

Clonal competition has been observed in different types of stem cells in earlier experiments (Klein and Simons, 2011; Hara et al., 2014; Nakagawa et al., 2007; Lopez-Garcia et al., 2010). It has observed that in clonal competition of mouse spermatogonial stem cells (activated with GFR α1 gene) the number of clones reduces with time, while average clone sizes increases with time (Hara et al., 2014). Similar qualitative behavior of stem cell has been observed in other different experimental studies as well (Klein and Simons, 2011; Nakagawa et al., 2007; Lopez-Garcia et al., 2010). In our model, to study clonal competition, we have taken the simplest case such as non-competitive competition (heterogeneous evolution of clones). In this competition, a stem cell stochastically divides and replaced by its daughter cells. We have started from 50 clones and observed that number of clones reduces with time and dominated by fewer clones (Figure 8A). These dominated clones (Figure 8B) increase their sizes with time. Figures 8C_1–8C_6 show the number of clones at different-different events, and each colored slice represents the size of the clone. So this supports the hypothesis that in clonal competition number of clones reduces with time and average clone size increases.

DISCUSSION

Maintenance of homeostasis results from a delicate balance between cellular proliferation and differentiation, and this diversity is regulated by key mechanisms which can be either intrinsic and niche. It is well known that stem cells are stochastically lost in tissue formation and replaced by daughter cells, although it is not understood how a cell decides to either keep the same identity or adapt to a new identity. Factors that play crucial role in cell fate decisions have been suggested and verified by experiments and here we examine these questions from a modeling perspective.

We propose a population-based stochastic cell division model having key components: nucleus position, segregation of transcription factors in daughter cells, and gene-regulatory network. The proposed model starts from a single stem cell which grows from an initial volume, with specific nucleus position and transcription factors, to a critical volume and divides. The growth is governed by a GRN, which is inherited by the daughter cells which can either be stem cells or differentiated cells. The GRN consists of three different attractors in which two correspond to differentiated and third represent stem state. Daughter cells also inherit transcription factors respective to their volumes. Inherent noise drives the stem cell to either retain or change its identity. In the model, we considered irreversible differentiation such that

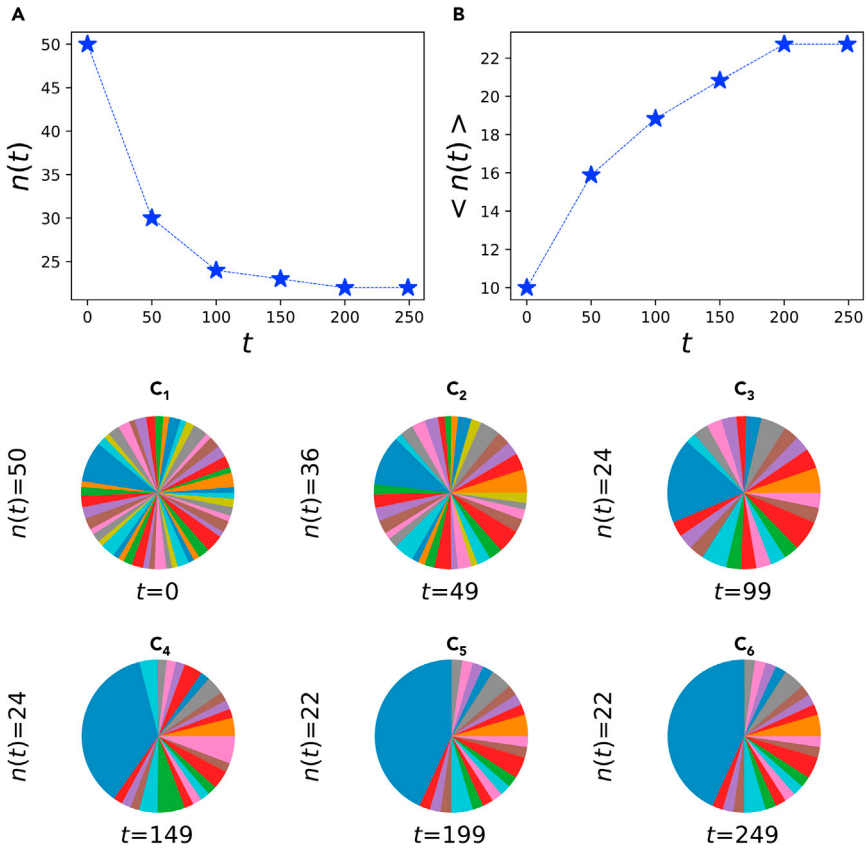

Figure 8. Heterogeneous evolution of clones

(A) displays decreasing behavior of clone numbers over event (time) showing that clonal competition is dominated by few clones.

(B) displays increase in average clone size over event (time).

(C_1–C_6) pie chart represents the number clones at different events where each slice is showing the size of individual clone.

differentiated cell can not retain stem cell property. Stochastic simulations that were carried out suggest that factors such as the nucleus position are important since biasing toward the apex makes cell division symmetric division, while biasing to the basal position leads to asymmetric division, which results in a greater proportion of differentiated cells. Asymmetric cell division takes longer time to reach up to a certain cell number while lesser time is taken by symmetric division. The model results are qualitatively in good agreement with experimental observations.

The stochasticity always remains an important aspect of generating phenotypic diversity either by activating or suppressing specific genes that ultimately leads to different or same cell commitment. The role of stochasticity has been studied well from experimental as well as modeling perspective (Elowitz et al., 2002; Maamar et al., 2007; Safdari et al., 2020; Hoffmann et al., 2008; Wang et al., 2007, 2015; Xu et al., 2016). Consistent with these studies, our model also confirms that stochasticity alone can generate phenotypic variability without cell-cell interaction and this variability is greatly affected by stochasticity due to low copy number of transcription factors in cells. Two principal types of genealogies have been experimentally observed in different cells which were intrinsically programmed: short and non-terminating (Qian et al., 1998, 2000). The model also provides similar types of genealogies driven by inherent noise. Along with inherent noise, we also explored different factors which can regulate the size of these genealogies. These factors may give deeper insight about the regulatory mechanism of controlling the size of genealogies. In the model, we observed that division plane can control the size of genealogies such as vertical division leads to more genealogies which are non-terminating because of symmetric division (self-renewal). On the other hand, asymmetric division provides more short genealogies with zero stem cells in horizontal division.

The role of division plane in cell fate decision is well studied which indirectly regulate symmetric and asymmetric division (Morrison and Kimble, 2006). The division plane is mainly controlled by the nucleus position which ultimately bias the cell fate (Ajduk et al., 2014). Such as in NDD model (Safdari et al., 2020), the deviation of division plane from central nuclei leads to more differentiated cells. And the fraction of these differentiated cells is high for low copy number of transcription factors and the fraction tend to be low for high copy number. To better understand how nucleus position bias the cell fate decision by regulating division plane, we consider different types of division plane which are controlled by nucleus and also explored the role of noisy nucleus. The model finds that nucleus position toward apex shows a pool of large stem cells due to symmetric division, whereas large differentiated cells are observed when nucleus moves to basal portion (compared with the center of cell). Introducing noise in the nucleus, we find that there are more symmetric differentiation which results in increased pool of differentiated cell in case of apex nuclei. In case of basal nuclei, more asymmetric differentiation has been observed resulting in more differentiated cells. This might provide an insight that Suitable interactions between the nucleus and transcription factors can regulate the balance between symmetric and asymmetric cell division. For example in developing tissue or wound healing process self-renewal is the prominent mechanism while adult tissues are maintained my asymmetric division (Morrison and Kimble, 2006). The model provides an insight that asymmetric cell division can be obtained by two factors basal nuclei and noise in the nucleus position. Interestingly, we observe an increasing pattern of cell population which is followed by decreasing pattern. Cell distribution in individual generation follows Gaussian distribution, which has been observed in the proliferation of B lymphocyte (Mitchell et al., 2018).

The present studies have focused on the role of internal noise, namely the intrinsic mechanism. Cell-cell communication is an influence in the niche mechanism and it will be important to study the effect of external noise in the model: the internal noise of one cell acts as an external source of noise for others. Another aspect that is important to explore is the role of dimensionality and the dependence of average clone size on on different tissue types (Klein and Simons, 2011). The minimal requirement for the number of attractors in the GRN is two, so it is likely that some of these results may be obtained with a simpler bistable switch, and this needs to be examined. We hope to pursue some of these directions in future work.

Limitations of the study

This study provides a mechanism of single cell division based on Waddington energy landscape which includes some key components. In this study, we considered only one type of synthetic GRN for each cell and did not include cell-cell interaction and also kept the noise level high, which have limitations in the interpretation of results. First, although the bimodal distribution of cell is independent form GRN type (Markov chain), changing the GRN may results in the different distributions. Second, changing the noise level may alter the fraction of symmetric and asymmetric cell division which may result in the different population of cells i.e. number of transitions from stem state to different state may reduce in presence of low noise. Third, in case of cell-cell interaction and different type of tissues, there is possibility of specific trend in the survival clones and average clone size.

STAR★METHODS

Detailed methods are provided in the online version of this paper and include the following:

- KEY RESOURCES TABLE
- RESOURCE AVAILABILITY
  - Lead contact
  - Materials availability
  - Data and code availability
- METHOD DETAILS
  - Rules of cell division
  - Markov chain
- QUANTIFICATION AND STATISTICAL ANALYSIS
  - Comparison of stochastic model versus Markov chain
  - Cell count for different plane of cleavage over nucleus position

SUPPLEMENTAL INFORMATION

Supplemental information can be found online at https://doi.org/10.1016/j.isci.2021.103199

ACKNOWLEDGMENTS

This work was supported by University Grants Commission of India (Grant number: 21/06/2015(i)EU-V) and JC Bose Fellowship by Department of Science and Technology India (Grant number: SR/S2/JCB-05/2008).

AUTHOR CONTRIBUTIONS

Conceptualization and methodology, A.J. and S.S.; analysis: A.J., S.S., and R.R.; writing - original draft: A.J.; writing - review & editing: A.J. and R.R.; supervision: R.R.

DECALARATION OF INTERESTS

The authors declare no competing interests.

Received: February 19, 2021
Revised: May 21, 2021
Accepted: September 28, 2021
Published: October 22, 2021

REFERENCES

Abrash, E.B., and Bergmann, D.C. (2009). Asymmetric cell divisions: a view from plant development. Dev. Cell *16*, 783–796.

Ajduk, A., Biswas Shivhare, S., and Zernicka-Goetz, M. (2014). The basal position of nuclei is one pre-requisite for asymmetric cell divisions in the early mouse embryo. Dev. Biol. *392*, 133–140.

Albertson, R., and Doe, C.Q. (2003). Dlg, Scrib and Lgl regulate neuroblast cell size and mitotic spindle asymmetry. Nat. Cell Biol. *5*, 166–170.

Berika, M., Elgayyar, M.E., and El-Hashash, A.H. (2014). Asymmetric cell division of stem cells in the lung and other systems. Front. Cell Dev. Biol. *2*, 33.

Betschinger, J., and Knoblich, J.A. (2004). Dare to be different: asymmetric cell division in Drosophila, C. elegans and vertebrates. Curr. Biol. *14*, R674–R685.

Broadus, J., and Doe, C.Q. (1997). Extrinsic cues, intrinsic cues and microfilaments regulate asymmetric protein localization in Drosophila neuroblasts. Curr. Biol. *7*, 827–835.

Caussinus, E., and Gonzalez, C. (2005). Induction of tumor growth by altered stem-cell asymmetric division in Drosophila melanogaster. Nat. Genet. *37*, 1125–1129.

Chang, H.H., Hemberg, M., Barahona, M., Ingber, D.E., and Huang, S. (2008). Transcriptome-wide noise controls lineage choice in mammalian progenitor cells. Nature *453*, 544–547.

Chen, C., Fingerhut, J.M., and Yamashita, Y.M. (2016). The ins(ide) and outs(ide) of asymmetric stem cell division. Curr. Opin. Cell Biol. *43*, 1–6.

Costa, M.R., Ortega, F., Brill, M.S., Beckervordersandforth, R., Petrone, C., Schroeder, T., Götz, M., and Berninger, B. (2011). Continuous live imaging of adult neural stem cell division and lineage progression in vitro. Development *138*, 1057–1068.

Delaunay, D., Cortay, V., Patti, D., Knoblauch, K., and Dehay, C. (2014). Mitotic spindle asymmetry: a Wnt/PCP-regulated mechanism generating asymmetrical division in cortical precursors. Cell Rep. *6*, 400–414.

Delaunay, D., Robini, M.C., and Dehay, C. (2015). Mitotic spindle asymmetry in rodents and primates: 2D vs. 3D measurement methodologies. Front. Cell. Neurosci. *9*, 33.

Doe, C.Q., and Bowerman, B. (2001). Asymmetric cell division: fly neuroblast meets worm zygote. Curr. Opin. Cell Biol. *13*, 68–75.

El-Hashash, A.H., and Warburton, D. (2011). Cell polarity and spindle orientation in the distal epithelium of embryonic lung. Dev. Dyn. *240*, 441–445.

Elowitz, M.B., Levine, A.J., Siggia, E.D., and Swain, P.S. (2002). Stochastic gene expression in a single cell. Science *297*, 1183–1186.

Enver, T., Pera, M., Peterson, C., and Andrews, P.W. (2009). Stem cell states, fates, and the rules of attraction. Cell Stem Cell *4*, 387–397.

Gardner, T.S., Cantor, C.R., and Collins, J.J. (2000). Construction of a genetic toggle switch in Escherichia coli. Nature *403*, 339–342.

Gönczy, P. (2002). Mechanisms of spindle positioning: focus on flies and worms. Trends Cell Biol. *12*, 332–339.

Götz, M., and Huttner, W.B. (2005). The cell biology of neurogenesis. Nat. Rev. Mol. Cell Biol. *6*, 777–788.

Grill, S.W., Gönczy, P., Stelzer, E.H., and Hyman, A.A. (2001). Polarity controls forces governing asymmetric spindle positioning in the Caenorhabditis elegans embryo. Nature *409*, 630–633.

Hara, K., Nakagawa, T., Enomoto, H., Suzuki, M., Yamamoto, M., Simons, B.D., and Yoshida, S. (2014). Mouse spermatogenic stem cells continually interconvert between equipotent singly isolated and syncytial states. Cell Stem Cell *14*, 658–672.

Hartfiel, D.J., and Seneta, E. (1994). On the theory of Markov set-chains. Adv. Appl. Probab. *26*, 947–964.

Hawkins, E.D., Markham, J.F., McGuinness, L.P., and Hodgkin, P.D. (2009). A single-cell pedigree analysis of alternative stochastic lymphocyte fates. Proc. Natl. Acad. Sci. U S A *106*, 13457–13462.

Haydar, T.F., Ang, E., and Rakic, P. (2003). Mitotic spindle rotation and mode of cell division in the developing telencephalon. Proc. Natl. Acad. Sci. U S A. *100*, 2890–2895.

Hoffmann, M., Chang, H.H., Huang, S., Ingber, D.E., Loeffler, M., and Galle, J. (2008). Noise-driven stem cell and progenitor population dynamics. PLoS One *3*, e2922.

Horvitz, H.R., and Herskowitz, I. (1992). Mechanisms of asymmetric cell division: two Bs or not two Bs, that is the question. Cell *68*, 237–255.

Huang, S., Eichler, G., Bar-Yam, Y., Ingber, D.E., and Ingber, D.E. (2005). Cell fates as high-dimensional attractor states of a complex gene regulatory network. Phys. Rev. Lett. *94*, 128701.

Huang, S., Guo, Y.P., May, G., and Enver, T. (2007). Bifurcation dynamics in lineage-commitment in bipotent progenitor cells. Dev. Biol. *305*, 695–713.

Inaba, M., and Yamashita, Y.M. (2012). Asymmetric stem cell division: precision for robustness. Cell Stem Cell *11*, 461–469.

Joseph, K., and Jessica, H. (2015). Introduction to Probability (CRC Press).

Kaltschmidt, J.A., Davidson, C.M., Brown, N.H., and Brand, A.H. (2000). Rotation and asymmetry of the mitotic spindle direct asymmetric cell division in the developing central nervous system. Nat. Cell Biol. *2*, 7–12.

Klein, A.M., and Simons, B.D. (2011). Universal patterns of stem cell fate in cycling adult tissues. Development *138*, 3103–3111.

Knoblich, J.A. (2001). Asymmetric cell division during animal development. Nat. Rev. Mol. Cell Biol. *2*, 11–20.

Konno, D., Shioi, G., Shitamukai, A., Mori, A., Kiyonari, H., Miyata, T., and Matsuzaki, F. (2008).

Neuroepithelial progenitors undergo LGN-dependent planar divisions to maintain self-renewability during mammalian neurogenesis. Nat. Cell Biol. *10*, 93–101.

Lai, K., Robertson, M.J., and Schaffer, D.V. (2004). The sonic hedgehog signaling system as a bistable genetic switch. Biophys. J. *86*, 2748–2757.

Lee, C.Y., Robinson, K.J., and Doe, C.Q. (2006). Lgl, Pins and aPKC regulate neuroblast self-renewal versus differentiation. Nature *439*, 594–598.

Li, C., Zhang, L., and Nie, Q. (2018). Landscape reveals critical network structures for sharpening gene expression boundaries. BMC Syst. Biol. *12*, 67.

Li, R. (2013). The art of choreographing asymmetric cell division. Dev. Cell *25*, 439–450.

Lopez-Garcia, C., Klein, A.M., Simons, B.D., and Winton, D.J. (2010). Intestinal stem cell replacement follows a pattern of neutral drift. Science *330*, 822–825.

Losick, R., and Desplan, C. (2008). Stochasticity and cell fate. Science *320*, 65–68.

Losick, V.P., Morris, L.X., Fox, D.T., and Spradling, A. (2011). Drosophila stem cell niches: a decade of discovery suggests a unified view of stem cell regulation. Dev. Cell *21*, 159–171.

Lu, T., Volfson, D., Tsimring, L., and Hasty, J. (2004). Cellular growth and division in the Gillespie algorithm. Syst. Biol. *1*, 121–128.

Maamar, H., Raj, A., and Dubnau, D. (2007). Noise in gene expression determines cell fate in Bacillus subtilis. Science *317*, 526–529.

Mitchell, S., Roy, K., Zangle, T.A., and Hoffmann, A. (2018). Nongenetic origins of cell-to-cell variability in B lymphocyte proliferation. Proc. Natl. Acad. Sci. U S A *115*, E2888–E2897.

Morrison, S.J., and Kimble, J. (2006). Asymmetric and symmetric stem-cell divisions in development and cancer. Nature *441*, 1068–1074.

Morrison, S.J., and Spradling, A.C. (2008). Stem cells and niches: mechanisms that promote stem cell maintenance throughout life. Cell *132*, 598–611.

Nakagawa, T., Nabeshima, Y., and Yoshida, S. (2007). Functional identification of the actual and potential stem cell compartments in mouse spermatogenesis. Dev. Cell *12*, 195–206.

Neumüller, A.,R., and Knoblich, J.A. (2009). Dividing cellular asymmetry: asymmetric cell division and its implications for stem cells and cancer. Genes Dev. *23*, 2675–2699.

Okuno, Y., Huang, G., Rosenbauer, F., Evans, E.K., Radomska, H.S., Iwasaki, H., Akashi, K., Moreau-Gachelin, F., Li, Y., and Zhang, P.e. a. (2005). Potential autoregulation of transcription factor PU.1 by an upstream regulatory element. Mol. Cell Biol. *25*, 2832–2845.

Perez-Carrasco, R., Barnes, C.P., Schaerli, Y., Isalan, M., Briscoe, J., and Page, K.M. (2018). Combining a toggle switch and a repressilator within the AC-DC circuit generates distinct dynamical behaviors. Cell Syst. *6*, 521–530.

Perez-Carrasco, R., Guerrero, P., Briscoe, J., and Page, K.M. (2016). Intrinsic noise profoundly alters the dynamics and steady state of morphogen-controlled bistable genetic switches. PLoS Comput. Biol. *12*, e1005154.

Pokhilko, A., Ebenhöh, O., Stark, M.W., and Colloms, S.D. (2018). Mathematical model of a serine integrase-controlled toggle switch with a single input. J. R. Soc. Interface *15*, 20180160.

Qian, X., Goderie, S.K., Shen, Q., Stern, J.H., and Temple, S. (1998). Intrinsic programs of patterned cell lineages in isolated vertebrate CNS ventricular zone cells. Development *125*, 3143–3152.

Qian, X., Shen, Q., Goderie, S.K., He, W., Capela, A., Davis, A.A., and Temple, S. (2000). Timing of CNS cell generation: a programmed sequence of neuron and glial cell production from isolated murine cortical stem cells. Neuron *28*, 69–80.

Roy, K., Mitchell, S., Liu, Y., Ohta, S., Lin, Y.S., Metzig, M.O., Nutt, S.L., and Hoffmann, A. (2019). A regulatory circuit controlling the dynamics of NFκB cRel transitions B cells from proliferation to plasma cell differentiation. Immunity *50*, 616–628.

Safdari, H., Kalirad, A., Picioreanu, C., Tusserkani, R., Goliaei, B., and Sadeghi, M. (2020). Noise-driven cell differentiation and the emergence of spatiotemporal patterns. PLoS One *15*, e0232060.

Serbanescu, D., Ojkic, N., and Banerjee, S. (2020). Nutrient-dependent trade-offs between ribosomes and division protein synthesis control bacterial cell size and growth. Cell Rep. *32*, 108183.

Shokhirev, M.N., Almaden, J., Davis-Turak, J., Birnbaum, H.A., Russell, T.M., Vargas, J.A., and Hoffmann, A. (2015). A multi-scale approach reveals that NF-κB cRel enforces a B-cell decision to divide. Mol. Syst. Biol. *11*, 783.

Stine, R.R., and Matunis, E.L. (2013). Stem cell competition: finding balance in the niche. Trends Cell Biol. *23*, 357–364.

Stockholm, D., Edom-Vovard, F., Coutant, S., Sanatine, P., Yamagata, Y., Corre, G., Le Guillou, L., Neildez-Nguyen, T.M., and Páldi, A. (2010). Bistable cell fate specification as a result of stochastic fluctuations and collective spatial cell behaviour. PLoS One *5*, e14441.

Tsai, S.F., Strauss, E., and Orkin, S.H. (1991). Functional analysis and in vivo footprinting implicate the erythroid transcription factor GATA-1 as a positive regulator of its own promoter. Genes Dev. *5*, 919–931.

Venkei, Z.G., and Yamashita, Y.M. (2018). Emerging mechanisms of asymmetric stem cell division. J. Cell Biol. *217*, 3785–3795.

Waddington, C. (1957). The Strategy of the Genes (George Allen and Unwin).

Wang, J., Zhang, J., Yuan, Z., and Zhou, T. (2007). Noise-induced switches in network systems of the genetic toggle switch. BMC Syst. Biol. *1*, 50.

Wang, P., Lü, J., and Yu, X. (2015). Colored noise induced bistable switch in the genetic toggle switch systems. IEEE/ACM Trans. Comput. Biol. Bioinform. *12*, 579–589.

Wodarz, A., and Huttner, W.B. (2003). Asymmetric cell division during neurogenesis in Drosophila and vertebrates. Mech. Dev. *120*, 1297–1309.

Xu, Y., Li, Y., Zhang, H., Li, X., and Kurths, J. (2016). The switch in a genetic toggle system with Lévy noise. Sci. Rep. *6*, 31505.

Yu, F., Kuo, C.T., and Jan, Y.N. (2006). Drosophila neuroblast asymmetric cell division: recent advances and implications for stem cell biology. Neuron *51*, 13–20.

Yuan, H., Chiang, C.Y., Cheng, J., Salzmann, V., and Yamashita, Y.M. (2012). Regulation of cyclin A localization downstream of Par-1 function is critical for the centrosome orientation checkpoint in Drosophila male germline stem cells. Dev. Biol. *361*, 57–67.

Zakrzewski, W., Dobrzyński, M., Szymonowicz, M., and Rybak, Z. (2019). Stem cells: past, present, and future. Stem Cell Res. Ther. *10*, 68.

Zhou, J.X., and Huang, S. (2011). Understanding gene circuits at cell-fate branch points for rational cell reprogramming. Trends Genet. *27*, 55–62.

STAR★METHODS

KEY RESOURCES TABLE

REAGENT or RESOURCE	SOURCE	IDENTIFIER
Software and algorithms		
Gillespie algorithm	(Lu et al., 2004)	https://digital-library.theiet.org/content/journals/10.1049/sb_20045016
Numpy 1.16.2	Numpy	https://numpy.org/
Scipy 1.2.1	Scipy	https://scipy.org
NetworkX 2.4	NetworkX	https://pypi.org/project/networkx/2.4/
Python 3.7.4	Python	https://python.org/
Custom code for simulation and analysis	This paper	https://github.com/AmitJangid/Cell-Division

RESOURCE AVAILABILITY

Lead contact

Further information and requests for resources and reagents should be directed to and will be fulfilled by the lead contact, Amit Jangid (amitjangid050@gmail.com).

Materials availability

This study did not generate new unique reagents.

Data and code availability

- All data produced in this study are included in the published article and its supplementary information, or are available from the lead contact upon request.
- The code generated during this study are available at GitHub https://github.com/AmitJangid/Cell-Division
- Any additional information required to reanalyze the data reported in this paper is available from the lead contact upon request.

METHOD DETAILS

Rules of cell division

The following is the process of cell division which consists varies steps:

1. **Gene regulatory network:** The gene regulatory network consists two transcription factors X, and Y which inhibit each other and activate itself. The system exhibits three different attractors, each corresponds to a different cell type.

$$\frac{dX}{dt} = \alpha_1 \frac{X^n}{1+X^n} + \beta_1 \frac{1}{1+Y^m} - \mu_X X \quad \text{(Equation 1)}$$

$$\frac{dY}{dt} = \alpha_2 \frac{Y^m}{1+Y^m} + \beta_2 \frac{1}{1+X^n} - \mu_Y Y \quad \text{(Equation 2)}$$

a) Type A ($X > Y$) b). Type B ($X < Y$) c). Type S ($X \approx Y$) X, and Y are concentration of transcription factors, $\alpha_1 = 0.6$, and $\alpha_2 = 0.6$ are autocrine parameters, $\beta_1 = 0.3$, and $\beta_2 = 0.3$ are paracrine parameters, $n = 3$, and $m = 3$ are hill coefficient, $\mu_X = 0.3$, and $\mu_Y = 0.3$ are death rates of transcription factors X, and Y respectively.

2. Initialize with nucleus position $P_0 \in (0, 1)$, volume V_0, and a tree with root S. We have fixed $V_0 = 2$ (initial volume of stem cell) through out the model.

3. Start with population of X_0 and Y_0 for regulatory network which corresponds to stem state (Step: A stochastic model of homeostasis: the roles of noise and nuclear positioning in deciding cell fate).
4. Simulate Gillespie algorithm for $V \rightarrow 2V_0$ with $V=V_0 exp^{\lambda t}$, where $\lambda = \frac{ln(2)}{10}$.
5. Partition during cell division (Plane of cleavage and segregation of transcription factors):
   (a) Pick the cell based on P (in the first step it will be P_0) value.
   (b) If $r_1 > P$: Horizontal division, else: Vertical division.
   (c) Divide the cell into two daughter cells with volume V_1, and V_2 as volume reaches up to $2V_0$. If division is horizontal division then $V_1 \propto P$ and $V_2 \propto (1\text{-}P)$, else $V_1 = V_2 = V/2$ (vertical division).
   (d) If $r_2 > \frac{V_1}{V_1+V_2}$ then one molecule of X will be going in cell V_2 else in V_1. Repeat the process upto number of molecules of X and similar for Y.
   (e) Track deterministic division time of each daughter cell by $T = T_0 + \frac{1}{\lambda} ln\left(\frac{2V_0}{V_i}\right)$. T_0 is birth time, $2V_0$ is the final volume (always 4 in this model), and V_i is the initial volume of that cell.
6. Normalize the nucleus position of daughter cells after each division.

Horizontal division case:

(a) If $P \leq 0.5$ then nucleus position for first cell is (say P_1) $\frac{1}{2}$ and for second other cell it is (say P_2) $\frac{P}{2(1-P)}$.
(b) If $P > 0.5$ then nucleus position for first cell is (say P_1) $\frac{3P-1}{2P}$ and for second cell it is (say P_2) $\frac{1}{2}$.

Vertical division case:

(a) No change in the nucleus position.

Introducing noise in nucleus position:

(a) For cell 1:

$P_1 = P_1$ + unifrom random number between $-\frac{min(P_1,1-P_1)}{2}$ to $\frac{max(P_1,1-P_1)}{2}$.

(b) For cell 2:

$P_2 = P_2$ + unifrom random number between $-\frac{min(P_2,1-P_2)}{2}$ to $\frac{max(P_2,1-P_2)}{2}$.

Note: Follow Step: A stochastic model of homeostasis: the roles of noise and nuclear positioning in deciding cell fateb to check horizontal or vertical division case in each division.

7. Convert population X, and Y into concentration by dividing volume V_1, and V_2 respectively. Update the tree by simulating ODEs for the cell type (to know which cell type it is).
8. After division track each cell [T+τ (next division time), T (birth time), V, P, X, Y, parent node, daughter node, daughter fate], and update genealogical tree.
9. Go to Step: A stochastic model of homeostasis: the roles of noise and nuclear positioning in deciding cell fate and repeat up to a desired generation or number of cell division.

Note: $r_1, r_2 \in (0,1)$ (Uniform random number)

Markov chain

In the Markov chain (Hartfiel and Seneta, 1994; Joseph and Jessica, 2015) (Figure S8) α is the transition probability from state q_i to state q_{i+1} when both daughter cells are stem. Correspondingly, β is the transition probability from state q_i to state q_{i-1} when the daughter cells are differentiated cells, and γ is the stay put transition probability which arises when one daughter cell is stem cell and the other is differentiated.

We have a set of states, $Q = \{q_0, q_1, q_2 \ldots q_k\}$, where $q_i (i \in (0,k))$ being a state having i number of stem cells and also $Q_0 = \{0,1,0 \ldots 0\}$ as we always start from a single stem cell. State q_0 and q_k are absorbing states such that it is impossible to leave these states ($\alpha, \beta, \gamma = 0.0, 0.0, 1.0$) and the transition probabilities from state i to j is $0 \ \forall \ j \neq i \pm 1$. So the transition probability matrix for the Markov model is as follows. $T = \begin{pmatrix} 1 & 0 & 0 & 0 & \cdots & 0 & 0 \\ \beta & \gamma & \alpha & 0 & \cdots & 0 & 0 \\ 0 & \beta & \gamma & \alpha & \cdots & 0 & 0 \\ 0 & 0 & \beta & \gamma & \cdots & 0 & 0 \\ \vdots & \vdots & \vdots & \ddots & \ddots & \alpha & 0 \\ 0 & 0 & 0 & 0 & \beta & \gamma & \alpha \\ 0 & 0 & 0 & 0 & 0 & 0 & 1 \end{pmatrix}$ where row and column represents states from q_0 to q_k. Probability being in state q_j from state q_i after n divisions is $P_{i+1,j+1}$ element of $T^n \ \forall \ i,j \in (0,k)$. In this model i is always fixed at 1 as we have started from single stem cell, so each element of second raw in the matrix T^n corresponds to the probability of getting state q_j ($j = 0 \ldots k$) from q_1 (having one stem cell). See Figure S8 for probability distribution for three different sets of parameter values.

QUANTIFICATION AND STATISTICAL ANALYSIS

Comparison of stochastic model versus Markov chain

The stochastic model has total 24 cases (Table S1) and for each case there are total N = 5000 samples. To compare the stochastic model with Markov chain three parameters, α, β, γ, are needed. These parameters are calculated from N samples i.e. α is the fraction of how many cells divide symmetrically (both daughter cells are stem), β is the fraction of how many cells divide symmetrically (both daughter cells are differentiated), and γ is the fraction of how many cells divide asymmetrically (one daughter as stem and another differentiated cell) (Figure 4 and S8 for α, β, γ). After finding values of α, β, γ, Markov chain was plotted. We fit a Gaussian for both model and find the values of mean (μ) and variance (σ) for comparison between the model. Scipy library was used for Kolmogorov-Smirnov test (Figure S7).

Cell count for different plane of cleavage over nucleus position

To find the cell count of different cells for different nucleus position and plane of cleavage. We calculated differentiated and stem cells as leaf nodes for different nucleus position for each plane of division (Figures 6A–6H). And for 6I-J how many cell divisions lead to symmetric fate from vertical division for mixed case with and without noise was calculated.